

Symmetry Defense Against CNN Adversarial Perturbation Attacks

Blerta Lindqvist
Aalto University

blerta.lindqvist@aalto.fi

Abstract

Convolutional neural network classifiers (CNNs) are susceptible to adversarial attacks that perturb original samples to fool classifiers such as an autonomous vehicle’s road sign image classifier. CNNs also lack invariance in the classification of symmetric samples because CNNs can classify symmetric samples differently. Considered together, the CNN lack of adversarial robustness and the CNN lack of invariance mean that the classification of symmetric adversarial samples can differ from their incorrect classification. Could symmetric adversarial samples revert to their correct classification? This paper answers this question by designing a symmetry defense that inverts or horizontally flips adversarial samples before classification against adversaries unaware of the defense. Against adversaries aware of the defense, the defense devises a Klein four symmetry subgroup that includes the horizontal flip and pixel inversion symmetries. The symmetry defense uses the subgroup symmetries in accuracy evaluation and the subgroup closure property to confine the transformations that an adaptive adversary can apply before or after generating the adversarial sample. Without changing the preprocessing, parameters, or model, the proposed symmetry defense counters the Projected Gradient Descent (PGD) and AutoAttack attacks with near-default accuracies for ImageNet. Without using attack knowledge or adversarial samples, the proposed defense exceeds the current best defense, which trains on adversarial samples. The defense maintains and even improves the classification accuracy of non-adversarial samples.

1. Introduction

Despite achieving state-of-the-art status in computer vision [27, 34], convolutional neural network classifiers (CNNs) lack adversarial robustness because they can classify imperceptibly perturbed samples incorrectly [13, 26, 42, 54]. One of the first and still undefeated defenses against adversarial perturbation attacks is adversarial train-



Figure 1. The flip symmetry defense against zero-knowledge adversaries reverts adversarial samples to their correct classification by horizontally flipping the samples before classification. The defense classifies non-adversarial samples in the same way.

ing (AT) [35, 42, 54], which uses adversarial samples in training. However, AT reliance on attack knowledge during training [42] is a significant drawback since such knowledge might not be available.

Although engineered to incorporate symmetries such as horizontal flipping, translations, and rotations, CNNs lack invariance with respect to these symmetries [22] in the classification of datasets such as ImageNet [18], CIFAR10 [33], MNIST [39]. As a result, CNNs can classify samples differently after they have been horizontally flipped, or even slightly shifted or rotated [5, 22]. Furthermore, CNNs only provide approximate translation invariance [5, 6, 22, 30] and are unable to learn invariances with respect to symmetries such as rotation and horizontal flipping with data augmentation [5, 6, 22].

Against adversarial perturbation attacks causing misclassification, CNNs’ lack of invariance can be beneficial. Since adversarial samples misclassify, CNNs’ lack of invariance can cause adversarial samples to classify differently from their incorrect classification after symmetry is applied to the samples. Aiming to classify adversarial samples correctly, we raise the question:

Can we design a robust defense against adversarial perturbation attacks that leverages CNNs’ lack of invariance with respect to symmetries?

To address this question, we design a novel symmetry defense that only uses symmetry to counter adversarial perturbation attacks. The proposed symmetry defense makes the following main contributions:

- The proposed symmetry defense uses no adversarial samples or attack knowledge. In contrast, the current best defense trains the classifier with adversarial samples.
- The symmetry defense counters zero-knowledge adversaries with near-default accuracies by using either the horizontal flip symmetry or an artificial pixel inversion symmetry. Results are shown in Table 1 and in Table 4 in Appendix A.
- The defense also counters perfect-knowledge adversaries with near-default accuracies, as shown in Table 3.
- The defense devises a symmetry subgroup for accuracy evaluation. The closure property of the subgroup limits the transformations that adversaries can apply before or after generating the adversarial samples, even if adversaries apply a sequence of subgroup symmetries.
- The proposed defense uses an artificial symmetry of pixel intensity inversion, as discussed in Section 5.3.2 and in Section 5.4. Thus, the defense applies to classifiers of datasets without inherent symmetries.
- The symmetry defense maintains the non-adversarial accuracy and even exceeds it against perfect-knowledge adversaries, as shown in Table 3.

2. Related Work and Background

Symmetry. A transformation that leaves an object invariant is called a symmetry of that object. Some examples of image symmetry transformations include rotation, horizontal flipping, and inversion [44]. We provide definitions related to symmetry groups in Appendix B.

2.1. Equivariance and Invariance in CNNs.

Equivariance. A function f is equivariant with respect to a class of transformations \mathcal{T} if $\forall T \in \mathcal{T}$ of input x , a corresponding transformation T' of the function output $f(x)$ can be found, such that $f(Tx) = T'f(x)$, according to [51].

Invariance. A function f is invariant with respect to a class of transformations \mathcal{T} if $f(Tx) = f(x), \forall T \in \mathcal{T}$, according to [51]. Invariance is a special case of equivariance where T' is the identity transformation. Invariant functions can be constructed by simply discarding information, thus limiting the functions and discarding relevant information [23].

Stacking equivariant mappings followed by an invariant map is a standard blueprint used in machine learning [7] for learning mappings that are invariant with regard to transformations [7, 29]. CNNs stack equivariant mappings followed by an invariant map in order to learn invariant mappings [7] with respect to symmetry transformations. CNNs use stacked convolution and pooling layers [25] to achieve translation equivariance. Convolutional layers are designed to be equivariant with respect to translations due to kernel sliding [24, 38]. Other layers, such as pooling in CNNs,

also support local translation invariance [7, 19, 25]. In addition, CNNs learn other symmetries, such as rotations and flips, by augmenting the dataset with samples transformed by these symmetries [34].

2.1.1 CNN Lack of Translation Equivariance

CNNs are engineered to be translation-equivariant. Translation invariance for image classification means that the position of an object in an image should not impact its classification. To achieve translation equivariance, CNNs have alternating layers of local feature extraction and pooling [7, 19, 25]. CNN convolutional layers [34, 37] are engineered to be equivariant to translation symmetries by computing feature maps over the translation symmetry group [24, 53]. The pooling layers of CNNs positioned after convolutional layers enable local invariance to translation [19] because the output of the pooling operation does not change when the position of features changes within the pooling region. Cohen and Welling [14] show that convolutional layers, pooling, arbitrary pointwise nonlinearities, batch normalization, and residual blocks are equivariant.

Although translation equivariance is encoded in the CNN architecture [19], studies suggest that translation equivariance in CNNs is not complete [5, 6, 22, 30, 58]. Engstrom et al. [22] find that CNNs are not invariant to even small translations or rotations. Azulay and Weiss [5] contend that aliasing effects caused by the subsampling of the convolutional stride make CNNs non-invariant. Zhang [58] proposes an anti-aliasing solution to counter the lack of translation invariance caused by max pooling, average pooling, and strides. Kayhan and Gemert [30] contend that image boundary effects cause CNNs to be not translation-invariant because they learn filters that respond to particular absolute locations. Bouchacourt et al. [6] claim that the translation invariance built into CNNs is approximate and that in ImageNet models, translation invariance is primarily learned from the data and enhanced by data augmentation.

2.1.2 CNN Data Augmentation Marginally Effective

Data augmentation is widely used to teach CNNs invariance with respect to non-translation symmetries such as rotations, horizontal flipping, and scaling. In CNNs, data augmentation supplements the dataset with additional samples obtained by applying symmetries to the original samples. For ImageNet, data augmentation can consist of a random crop, horizontal flip, color jitter, and color transforms of original images [21]. Previous work [40] has found that an AlexNet CNN model learns representations equivariant to flipping, scaling, and rotation symmetries.

Although data augmentation dominates as the method for CNNs to learn invariances with respect to non-translation symmetries [27], studies show that data aug-

mentation is only marginally effective [5, 6, 22] and not as effective as incorporating symmetries in the model architecture [14, 31]. The work in [5, 6, 22] shows that CNNs cannot learn invariances with data augmentation. Engstrom et al. [22] find that data augmentation with rotation and translation only marginally improves invariance in CIFAR10 [32] and ImageNet classifiers. Azulay and Weiss [5] find that data augmentation only enables invariance to symmetries of images that resemble dataset images. Bouchacourt et al. [6] claim that non-translation invariance is learned from the data independently of data augmentation, finding that the primary source of invariance is the training data and data augmentation only increases the invariances that have been learned.

2.1.3 Other Equivariance CNNs Approaches Have Dataset Limitation

Given the limitations of CNN equivariance, there have been several approaches to incorporate symmetry. Schmidt and Roth [51] learn image priors that are rotation-invariant and build rotation-equivariant and invariant descriptors of features. Invariant scattering CNNs [8, 52] construct representations with translation and rotation invariance using a cascade of wavelet decompositions and transforms. Anselmi et al. [2] theorize a hierarchical architecture with basic invariant moduli. Deep symmetry networks [24] generalize CNNs by forming feature maps over symmetry groups. Group equivariant convolutional neural networks [14, 15] use a new type of layer with G-convolutions that exploits discrete symmetry groups generated by translations, reflections, and rotations. Dieleman et al. [19] introduce four operations that can be combined to provide partial equivariance with respect to rotations by generating rotated and flipped images, allowing parameter sharing between the representations of different orientations. Zhou et al. [59] address the lack of equivariance in CNNs with respect to rotations using active rotating filters (ARFs) that rotate during convolution and result in feature maps with encoded location and orientation. Marcos et al. [43] propose rotation equivariant vector field networks that encode rotation equivariance, invariance, and covariance by applying filters at many orientations and recording the orientation with the highest score. Finzi et al. [23] construct convolutional layers that are equivariant with respect to transformations of any specific Lie group with a surjective exponential map. Romero and Cordonnier [49] formulate self-attention with equivariance to arbitrary symmetry groups by defining positional encodings invariant to the group transformations.

CNN architectures that handle symmetry better have only been shown to work for simple or synthetic datasets, not ImageNet. Schmidt and Roth [51] conduct experiments on MNIST [39] and a 30-image car dataset. In-

variant scattering CNNs [8, 52] report on MNIST [39] and texture datasets. Anselmi et al. [2] show results for a small face dataset. Deep symmetric networks [24] use MNIST [39] and the synthetic NORB dataset. Group equivariant convolutional networks [14] report on CIFAR10 [32] and MNIST [39]. Dieleman et al. [19] use the Plankton dataset of 30,336 images, the Galaxies dataset of 61,578 images, and the Massachusetts buildings dataset of 151 images. Zhou et al. [59] show results with rotated MNIST [36] and CIFAR10 [32]. Marcos et al. [43] show results with rotated MNIST [36], a small dataset of 15 Google Map images of cars, and a dataset of 20K cathedral images. Finzi et al. [23] apply their method on the rotated MNIST [36] dataset and the QM9 regression dataset of 134K small inorganic molecules. Romero and Cordonnier [49] show classification results with rotated MNIST [36], CIFAR10 [32] and a dataset of tumorous/non-tumorous images.

2.2 Adversarial Perturbation Attacks

Szegedy et al. [54] defined the problem of generating adversarial samples as starting from original samples and applying a small perturbation that results in misclassification. Szegedy et al. [54] formalized the generation of adversarial samples as a minimization of the sum of perturbation and adversarial loss. Following the minimization for attacks targeted at a specific adversarial label shown in Appendix C, most current attacks start with original samples and use the classifier gradient to generate adversarial samples [13, 42, 45].

PGD Attack. The PGD attack [35] is one of the strongest adversarial perturbation attacks. PGD is an iterative white-box attack with a parameter that defines the magnitude of the perturbation of each step. PGD starts from an initial sample point x_0 and then iteratively finds the perturbation of each step and projects the perturbation on an L_p -ball.

Auto-PGD Attack. Auto-PGD (APGD) [17] is a variant of PGD that varies the step size and can use two different loss functions to achieve a stronger attack.

Square Attack. The Square Attack [1] is a score-based, black-box attack based on local randomized square-shaped updates instead of being based on the classifier gradient.

Fast Adaptive Boundary The white-box Fast Adaptive Boundary attack (FAB) [16] aims to find the minimum perturbation needed to change the classification of an original sample. However, FAB does not scale to ImageNet because of the large number of dataset classes.

AutoAttack. AutoAttack [17] is a parameter-free ensemble of attacks that includes: APGD_{CE} and APGD_{DLR}, FAB [16] and Square Attack [1].

2.3. Adversarial Defenses

Adversarial Training. AT [35, 42, 54] is one of the first and few defenses that have not been defeated. AT works by training classifiers with adversarial samples that are labeled correctly. The robust PGD AT defense [42] is formulated as a robust optimization problem and is considered one of the most successful adversarial defenses [41]. Although AT is the best current defense, AT has drawbacks. AT necessitates advance attack knowledge, which is unrealistic. In addition, AT requires generating adversarial samples during training, which increases training time due to adversarial sample computation.

Failed Defenses. Many other defenses have been shown to fail against an adaptive adversary. For example, defensive distillation has been shown to be not robust to adversarial samples [10], many adversarial detection defenses have been bypassed [11, 12], obfuscated gradient defenses [3] and other defenses [55] have been circumvented.

Some defenses [4, 56, 57] have not been shown to work with the ImageNet dataset. Hendrycks et al. [28] only experiment with a 30-class ImageNet, while [48] examines the adverse effect of overfitting on robust AT.

Summary. Relevant to the proposed defense, we derive the following key points from the related work:

- Adversarial perturbation attacks are still an open problem as the best current defense, AT, requires knowledge of the attack.
- CNNs do not achieve full equivariance with respect to symmetries such as translation, horizontal flipping, and rotation despite being designed and trained with data augmentation to incorporate these symmetries.
- Studies that better incorporate symmetries into CNNs have yet to succeed for big datasets such as ImageNet.

3. Threat Model

We formulate the threat model based on the recommendations for adversarial defenses in [9]. The threat model consists of three cases in which the adversary knows the model and its parameters and conducts white-box attacks:

- **Zero-Knowledge Adversary.** The adversary is unaware of the symmetry defense.
- **Perfect-Knowledge Adversary.** The adversary is aware of the symmetry defense and adapts the attack.
- **Limited-Knowledge Adversary.** Based on [9], this threat only needs to be evaluated if the zero-knowledge attack fails and the perfect-knowledge attack succeeds. Since the symmetry defense succeeds against both zero-knowledge and perfect-knowledge adversaries, we do not evaluate the defense against limited-knowledge adversaries.

4. Experimental Setting

We evaluate the proposed symmetry defense against adversaries identified in the threat model based on [9] in Section 3. Our implementation is based on the robustness AT package implementation [21] for ImageNet [50] with the same ResNet50 [27] architecture and parameters. ImageNet [50] is a 1000-class dataset of over 1.2M training images and 50K testing images. The training parameters are the same as in [21]. Depending on the threat model and the defense symmetry, the training dataset is either the original dataset, the dataset of inverted original images, or the dataset of original and inverted original images. The ResNet50 [27] architecture model is trained with the stochastic gradient descent (SGD) optimizer with a momentum of 0.9, a learning rate decaying by a factor of 10 every 50 epochs, and a batch size of 256. The classifier takes as input images with [0, 1] pixel value ranges. Based on [21], the evaluation is done on logits, non-softmax output. The code for reproducing the experimental results is included in the supplementary material.

Models. We train the following models with the same preprocessing, parameters, model, and training as in [21]. The only difference is the training dataset:

M-Orig – original ImageNet images.

M-Invert – inverted ImageNet images.

M-Orig-Invert – original and inverted ImageNet images.

Default Data Augmentation. We use the same data augmentation as in [21] in the models we train: random resized crops, random horizontal flips, color jitter, and Fancy Principal Component Analysis (Fancy PCA) [34]. The Color-Jitter transform randomly changes the brightness, contrast, and saturation. Fancy PCA [34] is a form of data augmentation that changes the intensities of RGB channels in training images by performing PCA analysis on ImageNet [18] images and adding to every image multitudes of the principal components. The magnitudes are proportional to the eigenvalues and a random variable drawn from a Gaussian distribution with 0 mean and 0.05 standard deviation in [21].

PGD Attacks. We evaluate the proposed defense against L_2 and L_∞ PGD [35] attacks parameterized according to [21] for ImageNet with ϵ values of 0.5, 1.0, 2.0, 3.0 for L_2 attacks, and ϵ values of 4/255, 8/255, 16/255 for L_∞ attacks. All PGD [35] attacks have 100 steps, with a step perturbation value defined as the ratio of $2.5 \times \epsilon$ over the number of steps, following [21], and generated with the [21] robustness package. All PGD attacks are targeted, with the target label chosen uniformly at random among the labels other than the ground truth label.

AutoAttack attacks. We evaluate against APGD, and SquareAttack attacks with 1,000 random samples for each experiment based on [17] experiments with ImageNet. We do not evaluate against FAB because it does not scale to ImageNet because of the large number of ImageNet

classes [17]. All APGD attacks are targeted. Square Attack [1] is not targeted based on [1], with 10,000 queries, $p = 0.02$ for L_2 , and $p = 0.01$ for L_∞ . Square Attack [1] settings are based on settings for ImageNet in [1]. APGD_{CE} [17] and APGD_{DLR} [17] settings were based on attack settings for ImageNet in [17].

Tools. The defense was written using PyTorch [47]. PGD attacks were generated with the Robustness (Python Library) [21], AutoAttack attacks were generated with the IBM Adversarial Robustness 360 Toolbox (ART) [46].

5. The Proposed Symmetry Defense

The proposed symmetry defense is based on the lack of invariance of CNNs with respect to symmetry transformations. Following, f is the CNN classifier boundary function (not the CNN classification function), and T is the pixel intensity inversion symmetry. The f function is the function that results from the stacking of equivariant mappings in CNNs without the final invariant mapping, as explained in Section 2.1.

5.1. CNN classifier boundary function f lacks equivariance with respect to symmetries

As explained in Section 2.1.1 and in Section 2.1.2, CNN classification lacks invariance with respect to symmetries. The lack of invariance of CNN classification with respect to symmetries [5, 6, 22, 30] indicates the lack of equivariance of the CNN classifier boundary function f with respect to symmetries.

Intuitively, the lack of invariance of CNN classification with respect to symmetries means that CNN classifier boundaries near symmetric samples are not symmetric. Otherwise, if the CNN classifier boundaries were symmetric around symmetric samples, then symmetric samples would classify the same, and CNN classification would not lack invariance.

Formally, we base our reasoning on the definition of equivariance as $f(Tx) = T(fx)$, where f is the function that finds the classifier boundary and T is the symmetry transformation. For the CNN classifier boundary function f , equivariance with respect to T would mean that the CNN classifier boundary would be the same whether we apply f or T first. However, the lack of invariance of CNN classification with respect to symmetries [5, 6, 22, 30] indicates that $f(Tx) \neq T(fx)$. Otherwise, if $f(Tx) = T(fx)$, then the boundaries would be the same and CNN classification would not lack invariance.

We conclude that the CNN classifier boundary function f is not equivariant with respect to symmetries. Taking pixel inversion as an example T symmetry, Figure 2 shows that inverting all dataset samples and finding the classifier boundary do not commute with each-other, and would result in different class boundaries.

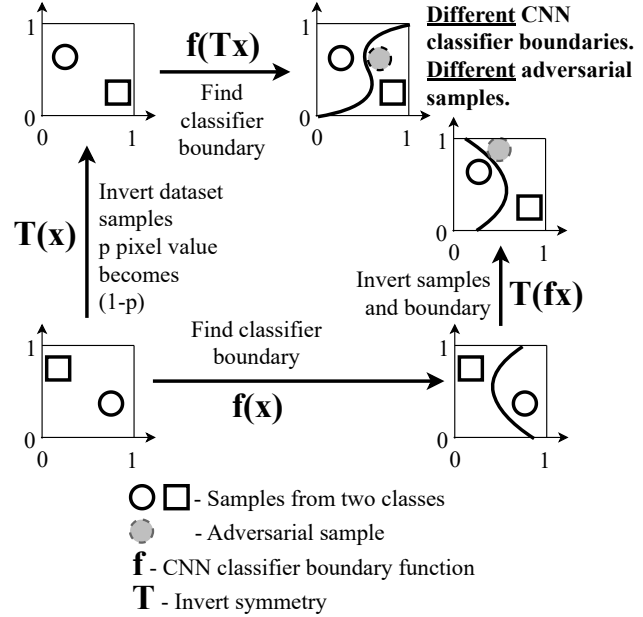


Figure 2. We show in two-dimensional space the inequivariance of the CNN classifier boundary function f with respect to the invert symmetry T . Applying first the inverse symmetry and then computing the classifier boundary function (up and right) produces a different boundary from computing the classifier function first and then applying the inverse symmetry (right and up). Due to the different class boundaries, adversarial perturbation finding is also not equivariant with respect to symmetries.

5.2. Adversarial Perturbation Finding Lacks Equivariance With Respect To Symmetries

The lack of equivariance of the CNN classifier function with respect to symmetries leads to the lack of equivariance of adversarial perturbation finding with respect to symmetry transformations. Conceptually, adversarial perturbation attacks [13, 26, 42, 45, 54] aim to change an original sample with a small perturbation in order to obtain an adversarial sample that is on the other side of the CNN classifier boundary and misclassifies as a result. Therefore, it stands to reason that different class boundaries in symmetric settings would cause an adversarial perturbation attack to find different adversarial perturbations, as Figure 2 shows.

5.3. Symmetry Defense Against Zero-Knowledge Adversaries

Following the threat model defined in Section 3, we evaluate the symmetry defense against zero-knowledge adversaries unaware of the defense and conduct non-adaptive attacks. We assume that zero-knowledge adversaries know the M-Orig model and its parameters and conduct white-box attacks. We discuss the flip symmetry defense in Section 5.3.1 and the intensity inversion symmetry defense in Section 5.3.2.

5.3.1 Horizontal Flipping Symmetry Defense Against Zero-Knowledge Adversaries

Here, we use the horizontal flip symmetry to counter zero-knowledge adversaries. Figure 3 outlines the flip symmetry defense against a zero-knowledge adversary. Table 1 shows the experimental results.

Figure 3 shows that the defense classifies an image by first horizontally flipping it and then classifying it with the same M-Orig model used by the adversary to generate the adversarial samples.

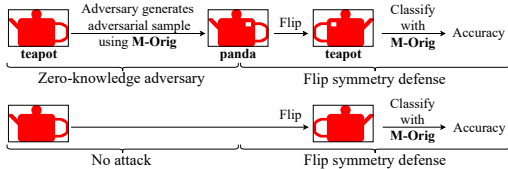


Figure 3. The flip symmetry defense against zero-knowledge adversaries reverts adversarial samples to their correct classification by horizontally flipping the samples before classification. The defense classifies non-adversarial samples in the same way. To classify samples, the defense uses the same M-Orig model that adversaries use to generate the adversarial samples.

Table 1. Accuracy evaluation of the flip symmetry defense against zero-knowledge adversaries.

Norm	Attack	No defense	Proposed defense
L_2	$\epsilon = 0.0$	77.26%	77.15%
	PGD - $\epsilon = 0.5$	34.27%	76.13%
	PGD - $\epsilon = 1.0$	4.32%	75.21%
	PGD - $\epsilon = 2.0$	0.19%	74.25%
	PGD - $\epsilon = 3.0$	0.03%	73.74%
	*APGD _{CE} - $\epsilon = 3.0$	0.00%	75.00%
	*APGD _{DLR} - $\epsilon = 3.0$	37.90%	79.20%
	*Square Attack - $\epsilon = 5.0$	40.00%	71.90%
	PGD - $\epsilon = 4/255$	0.00%	74.27%
	PGD - $\epsilon = 8/255$	0.00%	73.24%
L_∞	PGD - $\epsilon = 16/255$	0.00%	70.13%
	*APGD _{CE} - $\epsilon = 4/255$	0.00%	71.80%
	*APGD _{DLR} - $\epsilon = 4/255$	0.00%	78.70%
	*Square Attack - $\epsilon = 0.05$	4.90%	47.50%

*Evaluation based on 1,000 random samples.

The defense achieves close to the non-adversarial accuracy against most attacks, even exceeding it for APGD_{DLR}. Furthermore, the defense also exceeds the performance of the robust PGD AT defense [21] against PGD. The flip symmetry defense against a zero-knowledge adversary maintains the default non-adversarial accuracy.

5.3.2 Intensity Inversion Symmetry Defense Against Zero-Knowledge Adversaries

The intensity inversion symmetry that changes image pixel values from $p \in [0, 1]$ to $1 - p$ is not present in the image domain. Nevertheless, we use inversion symmetry to show that the proposed method can be employed in datasets without inherent symmetries. We train two models with the same preprocessing, parameters, and model architecture: M-Orig with original samples and M-Invert with inverted images. Figure 4 outlines the invert symmetry defense against a zero-knowledge adversary. The adversarial samples are generated by the adversary using the M-Orig model. The defense classifies a sample by inverting it and then classifying it with the M-Invert model.

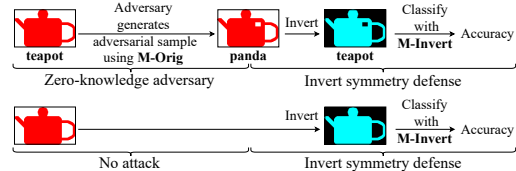


Figure 4. To revert adversarial samples generated with the M-Orig model to their correct classification, the invert symmetry defense against zero-knowledge adversaries inverts the samples before classifying them with the M-Invert model. The defense classifies non-adversarial samples in the same way.

The experimental results in Table 4 in Appendix A show that the inversion symmetry defense performs similarly to the flip symmetry defense, achieving near-default accuracies against most attacks and maintaining the non-adversarial accuracy.

5.4 Symmetry Defense Against Perfect-Knowledge Adversaries

According to the threat model defined in Section 3, we examine the symmetry defense against perfect-knowledge adversaries.

The defense needs more than one symmetry transformation to counter a perfect-knowledge adversary. The flip and invert symmetry defenses against zero-knowledge adversaries, discussed in Section 5.3.1 and Section 5.3.2, would not succeed against a perfect-knowledge adversary. The reason is that the adversary could apply the flip or invert symmetry after generating the adversarial sample, which would cancel out the symmetry transformation applied by the defense in Section 5.3 (flipping or inverting an image twice reverts it to the same image).

The defense against a perfect-knowledge adversary would need to use such symmetry transformations that their possible combinations are reasonably limited in number to enable the defense to conduct experiments for all cases. This rules out using rotations and translations because there are infinite possible rotations and translations.

Table 2. The Cayley table shows that the defined H subgroup is closed because all compositions of symmetries belong to the subgroup.

*	e	a	b	c
identity - e	e	a	b	c
flip - a	a	e	c	b
invert - b	b	c	e	a
flip and invert - c	c	b	a	e

Definition of the discrete subgroup of transformations. We define the discrete set of transformations $H = \{e, a, b, c\}$, where e, a, b, c denote the identity, horizontal flipping, intensity inversion, the composition of flipping and inversion. The operation $*$ means that one transformation follows another. The Cayley Table 2 shows that the subgroup is closed since compositions of the elements also belong to the subgroup. The defined H subgroup is known as the **Klein four-group**, a four-element group where each element is its own inverse and where composing any two non-identity elements results in the third non-identity element. Another way to define the Klein four-group H is: $H = \{a, b | a^2 = b^2 = (a * b)^2 = e\}$. Proof that H is a subgroup is in Appendix D.

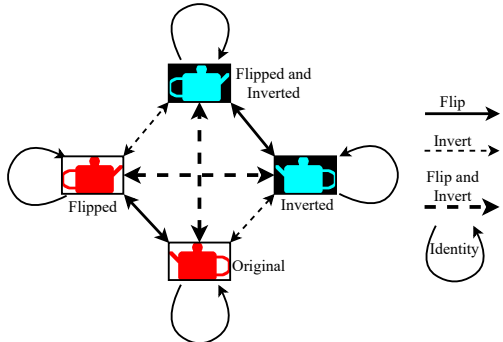


Figure 5. Here, we show that the symmetry subgroup limits the samples that a perfect-knowledge adversary can use to start from to generate the adversarial sample, even if the adversary applies a sequence of subgroup symmetries.

Training. Using data augmentation, we impose the H subgroup shown in Figure 5 on the M-Orig-Invert model by training it with original (identity), inverted original (inverting), horizontally flipped original (flipping), and horizontally flipped inverted samples (flipping and inverting).

Evaluation. The defense evaluates both original and adversarial samples in the same way. To classify a sample, the proposed defense applies all four symmetries to the sample and classifies all four samples with the M-Orig-Invert model. The defense assigns a class to the sample if the classification labels of two of the four symmetric samples agree. Evaluation with the proposed method is shown in Figure 6. Experimental results are shown in Table 3.

In Table 3, we evaluate the proposed defense against perfect-knowledge adversaries. The defense achieves near-default accuracies for many attacks, surpassing the current best defense, robust PGD AT defense [21], against PGD attacks. The defense also exceeds the default accuracy.

Adversary adaptability. We discuss how a perfect-knowledge adversary could adapt to the defense before, during, and after the generation of adversarial samples.

1) Before the adversarial generation. An adversary can choose to construct the adversarial sample starting from an original, flipped, inverted, or flipped and inverted sample, according to the H subgroup in Figure 5. We evaluate all four cases in Table 3. Furthermore, suppose the adversary applies a sequence of subgroup symmetries. In that case, the sequence is equivalent to a symmetry from the subgroup based on the closure property of the symmetry subgroup, shown in Figure 5.

2) During the adversarial perturbation generation. The adaptive adversary cannot adapt based on non-symmetry changes because the preprocessing, parameters, model architecture, and training do not change from [21]. In addition, the perfect-knowledge adversary needs to do more than find an adversarial sample to fool the defense because the defense does not classify based on only one sample. Instead, this adversary needs to find such an adversarial sample that at least two of its non-identity symmetry subgroup transformations also misclassify since the defense needs the classifications of two of the four subgroup symmetries to agree.

3) After the adversarial generation. After generating the adversarial sample, the adversary can apply any subgroup symmetries. However, this would be irrelevant because the defense applies all four subgroup symmetries to the sample. Due to the subgroup closure property, the set of four images that the defense obtains would be the same regardless of whether the adversary applies any sequence of subgroup symmetries after generating the adversarial sample.

5.5. Discussion of The Proposed Defense

The defense does not work for the smaller MNIST and CIFAR10 datasets. The reason could be the smaller sample dimensionality, number of samples, or number of classes in these datasets. Furthermore, MNIST lacks the horizontal flip symmetry used by the defense.

Computational resources. The proposed method has negligible computational overhead for the flip symmetry defense and roughly doubles the computational resources for the invert symmetry defense and the symmetry subgroup defense. Detailed computational analysis is in Appendix E.

Not a detection defense. The proposed defense is not a detection defense because it classifies original and adversarial samples in the same way, as shown in Figure 3, Figure 4, and Figure 6.

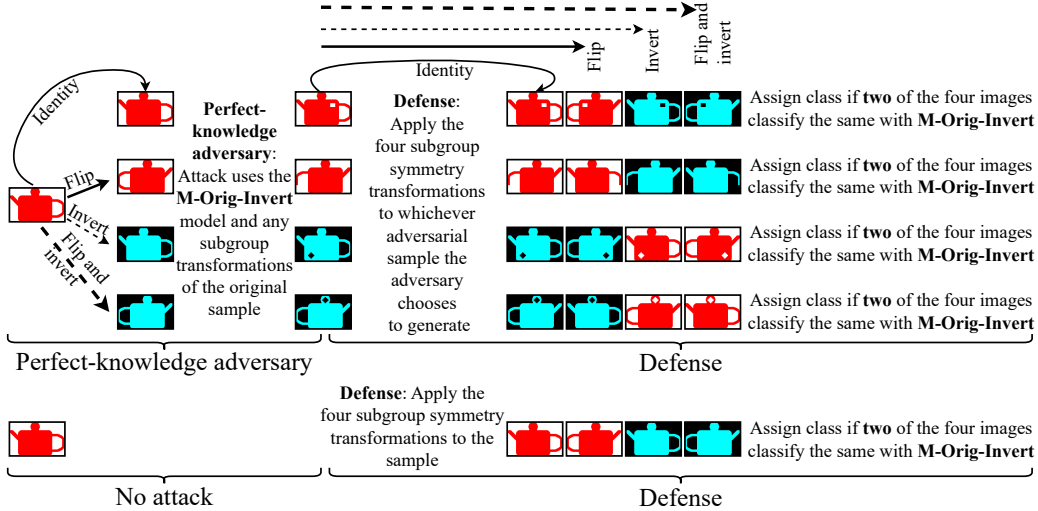


Figure 6. The symmetry subgroup defense against adaptive perfect-knowledge adversaries takes into consideration that symmetries could be applied to samples by adaptive adversaries both before and after adversarial generation. Moreover, even if adversaries applied consecutive subgroup symmetries to samples, they would not result in any other cases due to the closure property of the symmetry subgroup.

Table 3. Accuracy evaluation of the proposed symmetry defense against an adaptive perfect-knowledge adversary.

Norm	Attack	No defense	Proposed defense			
			Original	Flipped	Inverted	Flipped and Inverted
	$\epsilon = 0.0$	77.26%	78.30%	78.30%	78.30%	78.30%
L_2	PGD - $\epsilon = 0.5$	34.27%	75.65%	75.80%	75.72%	75.69%
	PGD - $\epsilon = 1$	4.32%	73.16%	73.27%	73.46%	73.35%
	PGD - $\epsilon = 2$	0.19%	70.80%	70.81%	70.80%	70.77%
	PGD - $\epsilon = 3$	0.03%	69.75%	69.82%	69.83%	69.89%
	*APGD _{CE} - $\epsilon = 3.0$	0.00%	70.50%	70.40%	71.00%	70.70%
	*APGD _{DLR} - $\epsilon = 3.0$	38.50%	77.70%	77.70%	78.00%	77.80%
	*SquareAttack - $\epsilon = 5.0$	43.00%	74.30%	74.50%	73.50%	73.10%
L_∞	PGD - $\epsilon = 4/255$	0.00%	70.68%	70.83%	70.77%	70.84%
	PGD - $\epsilon = 8/255$	0.00%	69.08%	69.12%	69.16%	69.21%
	PGD - $\epsilon = 16/255$	0.00%	65.26%	65.16%	65.32%	65.17%
	*APGD _{CE} - $\epsilon = 4/255$	0.00%	66.50%	66.90%	68.10%	66.60%
	*APGD _{DLR} - $\epsilon = 4/255$	0.60%	68.50%	68.10%	68.90%	69.40%
	*SquareAttack - $\epsilon = 0.05$	5.30%	49.00%	47.70%	48.70%	48.10%

*Evaluation based on 1,000 random samples.

The symmetry defense against perfect-knowledge adversaries exceeds the default accuracy and achieves near-default accuracies for many attacks. The defense also surpasses the robust PGD AT defense [21] against PGD attacks.

Not a gradient obfuscation defense. The defense does not rely on obfuscation because it keeps the exact preprocessing, parameters, and model as in [21].

6. Conclusions

The proposed symmetry defense succeeds with near-default accuracies against attacks ranging from being unaware of the defense to being aware of and adapting to it. The defense exceeds the classification accuracies of

the current best defense, which uses adversarial samples. The defense's non-reliance on attack knowledge or adversarial samples makes the defense applicable to realistic attack scenarios where the attack is unknown in advance. The defense's preservation of classifier preprocessing, parameters, architecture, and training facilitates the deployment of the defense to classifiers. The defense maintains the non-adversarial classification accuracy and even exceeds it against attacks aware of the defense.

References

- [1] Maksym Andriushchenko, Francesco Croce, Nicolas Flammarion, and Matthias Hein. Square attack: a query-efficient black-box adversarial attack via random search. In *Computer Vision–ECCV 2020: 16th European Conference, Glasgow, UK, August 23–28, 2020, Proceedings, Part XXIII*, pages 484–501. Springer, 2020. [3](#) [5](#)
- [2] Fabio Anselmi, Joel Z Leibo, Lorenzo Rosasco, Jim Mutch, Andrea Tacchetti, and Tomaso Poggio. Unsupervised learning of invariant representations in hierarchical architectures. *arXiv preprint arXiv:1311.4158*, 2013. [3](#)
- [3] Anish Athalye, Nicholas Carlini, and David Wagner. Obfuscated gradients give a false sense of security: Circumventing defenses to adversarial examples. *arXiv preprint arXiv:1802.00420*, 2018. [4](#)
- [4] Matan Atzmon, Niv Haim, Lior Yariv, Ofer Israelov, Haggai Maron, and Yaron Lipman. Controlling neural level sets. *Advances in Neural Information Processing Systems*, 32, 2019. [4](#)
- [5] Aharon Azulay and Yair Weiss. Why do deep convolutional networks generalize so poorly to small image transformations? *Journal of Machine Learning Research*, 20:1–25, 2019. [1](#) [2](#) [3](#) [5](#)
- [6] Diane Bouchacourt, Mark Ibrahim, and Ari Morcos. Grounding inductive biases in natural images: invariance stems from variations in data. *Advances in Neural Information Processing Systems*, 34:19566–19579, 2021. [1](#) [2](#) [3](#) [5](#)
- [7] Michael M Bronstein, Joan Bruna, Taco Cohen, and Petar Veličković. Geometric deep learning: Grids, groups, graphs, geodesics, and gauges. *arXiv preprint arXiv:2104.13478*, 2021. [2](#)
- [8] Joan Bruna and Stéphane Mallat. Invariant scattering convolution networks. *IEEE transactions on pattern analysis and machine intelligence*, 35(8):1872–1886, 2013. [3](#)
- [9] Nicholas Carlini, Anish Athalye, Nicolas Papernot, Wieland Brendel, Jonas Rauber, Dimitris Tsipras, Ian Goodfellow, Aleksander Madry, and Alexey Kurakin. On evaluating adversarial robustness. *arXiv preprint arXiv:1902.06705*, 2019. [4](#)
- [10] Nicholas Carlini and David Wagner. Defensive distillation is not robust to adversarial examples. *arXiv preprint arXiv:1607.04311*, 2016. [4](#)
- [11] Nicholas Carlini and David Wagner. Adversarial examples are not easily detected: Bypassing ten detection methods. In *Proceedings of the 10th ACM Workshop on Artificial Intelligence and Security*, pages 3–14. ACM, 2017. [4](#)
- [12] Nicholas Carlini and David Wagner. Magnet and “efficient defenses against adversarial attacks” are not robust to adversarial examples. *arXiv preprint arXiv:1711.08478*, 2017. [4](#)
- [13] Nicholas Carlini and David Wagner. Towards evaluating the robustness of neural networks. In *2017 IEEE Symposium on Security and Privacy (SP)*, pages 39–57. IEEE, 2017. [1](#) [3](#) [5](#)
- [14] Taco Cohen and Max Welling. Group equivariant convolutional networks. In *International conference on machine learning*, pages 2990–2999. PMLR, 2016. [2](#) [3](#)
- [15] Taco S Cohen, Mario Geiger, and Maurice Weiler. A general theory of equivariant cnns on homogeneous spaces. *Advances in neural information processing systems*, 32, 2019. [3](#)
- [16] Francesco Croce and Matthias Hein. Minimally distorted adversarial examples with a fast adaptive boundary attack. In *International Conference on Machine Learning*, pages 2196–2205. PMLR, 2020. [3](#)
- [17] Francesco Croce and Matthias Hein. Reliable evaluation of adversarial robustness with an ensemble of diverse parameter-free attacks. In *International conference on machine learning*, pages 2206–2216. PMLR, 2020. [3](#) [4](#) [5](#)
- [18] Jia Deng, Wei Dong, Richard Socher, Li-Jia Li, Kai Li, and Li Fei-Fei. Imagenet: A large-scale hierarchical image database. In *2009 IEEE conference on computer vision and pattern recognition*, pages 248–255. Ieee, 2009. [1](#) [4](#)
- [19] Sander Dieleman, Jeffrey De Fauw, and Koray Kavukcuoglu. Exploiting cyclic symmetry in convolutional neural networks. In *International conference on machine learning*, pages 1889–1898. PMLR, 2016. [2](#) [3](#)
- [20] David Steven Dummit and Richard M Foote. *Abstract algebra*, volume 3. Wiley Hoboken, 2004. [12](#)
- [21] Logan Engstrom, Andrew Ilyas, Hadi Salman, Shibani Santurkar, and Dimitris Tsipras. Robustness (python library), 2019. [2](#) [4](#) [5](#) [6](#) [7](#) [8](#) [12](#)
- [22] Logan Engstrom, Brandon Tran, Dimitris Tsipras, Ludwig Schmidt, and Aleksander Madry. Exploring the landscape of spatial robustness. In *International conference on machine learning*, pages 1802–1811. PMLR, 2019. [1](#) [2](#) [3](#) [5](#)
- [23] Marc Finzi, Samuel Stanton, Pavel Izmailov, and Andrew Gordon Wilson. Generalizing convolutional neural networks for equivariance to lie groups on arbitrary continuous data. In *International Conference on Machine Learning*, pages 3165–3176. PMLR, 2020. [2](#) [3](#)
- [24] Robert Gens and Pedro M Domingos. Deep symmetry networks. *Advances in neural information processing systems*, 27, 2014. [2](#) [3](#)
- [25] Ian Goodfellow, Honglak Lee, Quoc Le, Andrew Saxe, and Andrew Ng. Measuring invariances in deep networks. *Advances in neural information processing systems*, 22, 2009. [2](#)
- [26] Ian J Goodfellow, Jonathon Shlens, and Christian Szegedy. Explaining and harnessing adversarial examples. *arXiv preprint arXiv:1412.6572*, 2014. [1](#) [5](#)
- [27] Kaiming He, Xiangyu Zhang, Shaoqing Ren, and Jian Sun. Deep residual learning for image recognition. In *Proceedings of the IEEE conference on computer vision and pattern recognition*, pages 770–778, 2016. [1](#) [2](#) [4](#)
- [28] Dan Hendrycks, Kimin Lee, and Mantas Mazeika. Using pre-training can improve model robustness and uncertainty. In *International Conference on Machine Learning*, pages 2712–2721. PMLR, 2019. [4](#)
- [29] Irina Higgins, Sébastien Racanière, and Danilo Rezende. Symmetry-based representations for artificial and biological general intelligence. *Frontiers in Computational Neuroscience*, page 28, 2022. [2](#)

[30] Osman Semih Kayhan and Jan C van Gemert. On translation invariance in cnns: Convolutional layers can exploit absolute spatial location. In *Proceedings of the IEEE/CVF Conference on Computer Vision and Pattern Recognition*, pages 14274–14285, 2020. [1](#), [2](#), [5](#)

[31] Jonas Köhler, Leon Klein, and Frank Noé. Equivariant flows: exact likelihood generative learning for symmetric densities. In *International conference on machine learning*, pages 5361–5370. PMLR, 2020. [3](#)

[32] Alex Krizhevsky and Geoffrey Hinton. Learning multiple layers of features from tiny images. Master’s thesis, University of Toronto, 2009. [3](#)

[33] Alex Krizhevsky, Vinod Nair, and Geoffrey Hinton. Cifar-10 and cifar-100 datasets. *URL: <https://www.cs.toronto.edu/~kriz/cifar.html>*, 6, 2009. [1](#)

[34] Alex Krizhevsky, Ilya Sutskever, and Geoffrey E Hinton. Imagenet classification with deep convolutional neural networks. *Advances in neural information processing systems*, 25, 2012. [1](#), [2](#), [4](#)

[35] Alexey Kurakin, Ian Goodfellow, and Samy Bengio. Adversarial machine learning at scale. *arXiv preprint arXiv:1611.01236*, 2016. [1](#), [3](#), [4](#)

[36] Hugo Larochelle, Dumitru Erhan, Aaron Courville, James Bergstra, and Yoshua Bengio. An empirical evaluation of deep architectures on problems with many factors of variation. In *Proceedings of the 24th international conference on Machine learning*, pages 473–480, 2007. [3](#)

[37] Yann LeCun, Yoshua Bengio, et al. Convolutional networks for images, speech, and time series. *The handbook of brain theory and neural networks*, 3361(10):1995, 1995. [2](#)

[38] Yann LeCun, Bernhard Boser, John S Denker, Donnie Henderson, Richard E Howard, Wayne Hubbard, and Lawrence D Jackel. Backpropagation applied to handwritten zip code recognition. *Neural computation*, 1(4):541–551, 1989. [2](#)

[39] Yann LeCun, Corinna Cortes, and Christopher JC Burges. The mnist database of handwritten digits, 1998. *URL <http://yann.lecun.com/exdb/mnist>*, 10:34, 1998. [1](#), [3](#)

[40] Karel Lenc and Andrea Vedaldi. Understanding image representations by measuring their equivariance and equivalence. In *Proceedings of the IEEE conference on computer vision and pattern recognition*, pages 991–999, 2015. [2](#)

[41] Blerta Lindqvist. A novel method for function smoothness in neural networks. *IEEE Access*, 10:75354–75364, 2022. [4](#)

[42] Aleksander Madry, Aleksandar Makelov, Ludwig Schmidt, Dimitris Tsipras, and Adrian Vladu. Towards deep learning models resistant to adversarial attacks. *arXiv preprint arXiv:1706.06083*, 2017. [1](#), [3](#), [4](#), [5](#)

[43] Diego Marcos, Michele Volpi, Nikos Komodakis, and Devis Tuia. Rotation equivariant vector field networks. In *Proceedings of the IEEE International Conference on Computer Vision*, pages 5048–5057, 2017. [3](#)

[44] Willard Miller. *Symmetry groups and their applications*. Academic Press, 1973. [2](#)

[45] Seyed-Mohsen Moosavi-Dezfooli, Alhussein Fawzi, and Pascal Frossard. Deepfool: a simple and accurate method to fool deep neural networks. In *Proceedings of the IEEE conference on computer vision and pattern recognition*, pages 2574–2582, 2016. [3](#), [5](#)

[46] Maria-Irina Nicolae, Mathieu Sinn, Minh Ngoc Tran, Beat Bueser, Ambrish Rawat, Martin Wistuba, Valentina Zantedeschi, Nathalie Baracaldo, Bryant Chen, Heiko Ludwig, Ian Molloy, and Ben Edwards. Adversarial robustness toolbox v1.0.1. *CoRR*, 1807.01069, 2018. [5](#)

[47] Adam Paszke, Sam Gross, Francisco Massa, Adam Lerer, James Bradbury, Gregory Chanan, Trevor Killeen, Zeming Lin, Natalia Gimelshein, Luca Antiga, Alban Desmaison, Andreas Kopf, Edward Yang, Zachary DeVito, Martin Raison, Alykhan Tejani, Sasank Chilamkurthy, Benoit Steiner, Lu Fang, Junjie Bai, and Soumith Chintala. Pytorch: An imperative style, high-performance deep learning library. In H. Wallach, H. Larochelle, A. Beygelzimer, F. d’Alché-Buc, E. Fox, and R. Garnett, editors, *Advances in Neural Information Processing Systems 32*, pages 8024–8035. Curran Associates, Inc., 2019. [5](#)

[48] Leslie Rice, Eric Wong, and Zico Kolter. Overfitting in adversarially robust deep learning. In *International Conference on Machine Learning*, pages 8093–8104. PMLR, 2020. [4](#)

[49] David W Romero and Jean-Baptiste Cordonnier. Group equivariant stand-alone self-attention for vision. In *International Conference on Learning Representations*, 2020. [3](#)

[50] Olga Russakovsky, Jia Deng, Hao Su, Jonathan Krause, Sanjeev Satheesh, Sean Ma, Zhiheng Huang, Andrej Karpathy, Aditya Khosla, Michael Bernstein, et al. Imagenet large scale visual recognition challenge. *International journal of computer vision*, 115(3):211–252, 2015. [4](#)

[51] Uwe Schmidt and Stefan Roth. Learning rotation-aware features: From invariant priors to equivariant descriptors. In *2012 IEEE Conference on Computer Vision and Pattern Recognition*, pages 2050–2057. IEEE, 2012. [2](#), [3](#)

[52] Laurent Sifre and Stéphane Mallat. Rotation, scaling and deformation invariant scattering for texture discrimination. In *Proceedings of the IEEE conference on computer vision and pattern recognition*, pages 1233–1240, 2013. [3](#)

[53] Jure Sokolic, Raja Giryes, Guillermo Sapiro, and Miguel Rodrigues. Generalization error of invariant classifiers. In *Artificial Intelligence and Statistics*, pages 1094–1103. PMLR, 2017. [2](#)

[54] Christian Szegedy, Wojciech Zaremba, Ilya Sutskever, Joan Bruna, Dumitru Erhan, Ian J. Goodfellow, and Rob Fergus. Intriguing properties of neural networks. In *International Conference on Learning Representations*, 2013. [1](#), [3](#), [4](#), [5](#), [12](#)

[55] Florian Tramer, Nicholas Carlini, Wieland Brendel, and Aleksander Madry. On adaptive attacks to adversarial example defenses. *Advances in Neural Information Processing Systems*, 33:1633–1645, 2020. [4](#)

[56] Chang Xiao, Peilin Zhong, and Changxi Zheng. Enhancing adversarial defense by k-winners-take-all. In *International Conference on Learning Representations*, 2020. [4](#)

[57] Haichao Zhang and Jianyu Wang. Defense against adversarial attacks using feature scattering-based adversarial training. *Advances in Neural Information Processing Systems*, 32, 2019. [4](#)

- [58] Richard Zhang. Making convolutional networks shift-invariant again. In *International conference on machine learning*, pages 7324–7334. PMLR, 2019. [2](#)
- [59] Yanzhao Zhou, Qixiang Ye, Qiang Qiu, and Jianbin Jiao. Oriented response networks. In *Proceedings of the IEEE Conference on Computer Vision and Pattern Recognition*, pages 519–528, 2017. [3](#)

Appendices

A. Experimental Results of the Invert Symmetry Defense

Table 4. Accuracy evaluation of the invert symmetry defense against zero-knowledge adversaries.

Norm	Attack	No defense symmetry	Proposed defense
	$\epsilon = 0.0$	77.26%	76.88%
L_2	PGD - $\epsilon = 0.5$	34.27%	75.87%
	PGD - $\epsilon = 1.0$	4.32%	75.10%
	PGD - $\epsilon = 2.0$	0.19%	74.33%
	PGD - $\epsilon = 3.0$	0.03%	74.02%
	*APGD _{CE} - $\epsilon = 3.0$	0.00%	73.80%
	*APGD _{DLR} - $\epsilon = 3.0$	34.60%	76.00%
	*Square Attack - $\epsilon = 5.0$	40.40%	72.60%
L_∞	PGD - $\epsilon = 4/255$	0.00%	74.54%
	PGD - $\epsilon = 8/255$	0.00%	73.83%
	PGD - $\epsilon = 16/255$	0.00%	72.08%
	*APGD _{CE} - $\epsilon = 4/255$	0.00%	69.80%
	*APGD _{DLR} - $\epsilon = 4/255$	0.20%	71.20%
	*Square Attack - $\epsilon = 0.05$	4.00%	48.10%

*Evaluation based on 1,000 random samples.

Similarly to the flip symmetry defense, the invert symmetry defense achieves near-default accuracy against most attacks, exceeding the performance of the robust PGD AT defense [21] for PGD attacks. In addition, the defense accuracy decreases by 0.38 % points for non-adversarial samples, exceeding the PGD AT defense [21].

B. Definitions Related to Symmetry Groups

According to [20], a group is an ordered pair $(G, *)$ where G is a set and $*$ is a binary operation on G that satisfies these axioms:

- **Associativity.** $*$ is associative: $\forall a, b, c \in G, (a * b) * c = a * (b * c)$.
- **Identity.** There exists an identity element $e \in G$, such that $a * e = e * a = a$, for $\forall a \in G$.
- **Inverse.** Every element in G has an inverse: $\forall a \in G$, there exists $a^{-1} \in G$ such that $a * a^{-1} = a^{-1} * a = e$.

Binary Operation. According to [20], a binary operation $*$ on a set G is a function $*: G \times G \mapsto G$. Instead of writing the binary operation $*$ on $a, b \in G$ as a function $*(a, b)$, we can write it as $a * b$.

Closure. Suppose that $*$ is a binary operation on the set G and H is a subset of G . If $*$ is a binary operation on H , that is, $\forall a, b \in H, a * b \in H$, then H is said to be closed under the $*$ binary operation [20].

Group. According to [20], a group is an ordered pair $(G, *)$ where G is a set and $*$ is a binary operation on G that satisfies the associativity, identity and inverse axioms.

Subgroup. According to [20], a subset H of G is a subgroup of G if H is nonempty and H is closed under products and inverses (that is, $x, y \in H$ implies that $x^{-1} \in H$ and $x * y \in H$). A subgroup H of group G is written as $H \leq G$. Informally, the subgroup of a group G is a subset of G , which is itself a group with respect to the binary operation defined in G .

The Subgroup Criterion. A subset H of a group G is a subgroup if and only if $H \neq \emptyset$ and $\forall x, y \in H, x * y^{-1} \in H$ [20].

The Finite Subgroup Criterion. A finite subset H is a subgroup if H is nonempty and closed under $*$ [20].

C. The minimization of targeted adversarial perturbation attacks

The minimization for adversarial perturbation attacks targeted at a specific adversarial label was first formulated by Szegedy et al. [54]:

$$\begin{aligned} & \text{minimize} && c \cdot \|\delta\| + \text{loss}_f(x + \delta, l) \\ & \text{such that} && x + \delta \in [0, 1]^d, \end{aligned} \quad (1)$$

where f is the classifier function, loss_f is the classifier function loss, and l is an adversarial label, c is a constant, $\|\delta\|$ is the L_p norm of perturbation.

D. Proof That The Subgroup Transformations Form A Subgroup

Theorem. $H = \{e, a, b, c\}$ is a subgroup of the group of symmetry transformations of images.

Proof. Based on the finite subgroup criterion in Section 2, a finite subset of a group should need only to be nonempty and closed under operation $*$ [20]. H is nonempty because it has four elements and is a subset of the symmetry transformations of images. Based on the definition of closure in Section 2, for H to be closed under the $*$ operation, we need to show that $\forall a, b \in H$, we get that $a * b^{-1} \in H$. Table 2 shows that $\forall a, b \in H$, we get that $a * b \in H$. Table 2 also shows that each element is its own inverse element because $\forall b \in H$, we get $b * b = e$, which means that $b = b^{-1}$. From $\forall a, b \in H, a * b \in H$ and $\forall b \in H, b = b^{-1}$, we derive that $\forall a, b \in H, a * b^{-1} \in H$. \square

E. Computational Resources

Here, we analyze the additional computational complexity of the proposed defense and the adversary.

E.1. Defense

Against a zero-knowledge adversary. The flip symmetry defense uses the same computational complexity as a default classifier in training because it only trains one model with original samples. The invert symmetry defense doubles the computational complexity of a default classifier in training because it trains two models with original and inverted images, respectively. In testing, there is $O(1)$ overhead per sample due to flipping or inverting the sample.

Against a perfect-knowledge adversary. The symmetry subgroup defense doubles the computational complexity of a default classifier in training because it trains one model with both original and inverted images. In testing, there is $O(1)$ overhead per sample due to flipping, inverting, or flipping and inverting the sample.

E.2. Adversary

Zero-knowledge adversary. The zero-knowledge adversary is unaware of the defense and consumes the same resources as in the default case.

Perfect-knowledge adversary. The perfect-knowledge adversary can symmetrically transform the sample before and after generating the adversarial sample, using $O(1)$ additional computing resources per sample.